

## Carrier transport in $\text{In}_x\text{Ga}_{1-x}\text{N}$ thin films grown by modified activated reactive evaporation

S. R. Meher, R. V. Muniswami Naidu, Kuyyadi P. Biju, A. Subrahmanyam, and Mahaveer K. Jain

Citation: [Applied Physics Letters](#) **99**, 082112 (2011); doi: 10.1063/1.3630000

View online: <http://dx.doi.org/10.1063/1.3630000>

View Table of Contents: <http://scitation.aip.org/content/aip/journal/apl/99/8?ver=pdfcov>

Published by the [AIP Publishing](#)

---

### Articles you may be interested in

[Effect of disorder on carrier transport in ZnO thin films grown by atomic layer deposition at different temperatures](#)  
J. Appl. Phys. **114**, 043703 (2013); 10.1063/1.4815941

[Dependence on composition of the optical polarization properties of m-plane  \$\text{In}\_x\text{Ga}\_{1-x}\text{N}\$  commensurately grown on ZnO](#)  
Appl. Phys. Lett. **99**, 061912 (2011); 10.1063/1.3624462

[The electronic properties of amorphous and crystallized  \$\text{In}\_2\text{O}\_3\$  films](#)  
J. Appl. Phys. **100**, 093706 (2006); 10.1063/1.2358829

[Spectroscopic characterization of 1.3  \$\mu\text{m}\$  GaInNAs quantum-well structures grown by metal-organic vapor phase epitaxy](#)  
Appl. Phys. Lett. **86**, 092106 (2005); 10.1063/1.1868866

[Electron transport in In-rich  \$\text{In}\_x\text{Ga}\_{1-x}\text{N}\$  films](#)  
J. Appl. Phys. **97**, 046101 (2005); 10.1063/1.1847694

---



## Carrier transport in $\text{In}_x\text{Ga}_{1-x}\text{N}$ thin films grown by modified activated reactive evaporation

S. R. Meher, R. V. Muniswami Naidu, Kuyyadi P. Biju,<sup>a)</sup> A. Subrahmanyam, and Mahaveer K. Jain<sup>b)</sup>

Department of Physics, Indian Institute of Technology, Madras, Chennai-600036, India

(Received 30 May 2011; accepted 8 August 2011; published online 26 August 2011)

In the present work, we report the temperature dependent carrier transport properties of  $\text{In}_x\text{Ga}_{1-x}\text{N}$  thin films in the entire composition range grown by modified activated reactive evaporation. The carrier transport in these degenerate semiconductors is controlled by impurity band conduction. A transition from metallic to semiconducting type resistivity was observed for indium rich films. The semiconducting behavior originates from electron–electron interaction and weak localization, whereas higher temperature scattering contributes to the metallic type resistivity. A transition of resistivity behavior from the quantum phenomena to the classical Arrhenius approach was observed for  $x=0.12$  film. © 2011 American Institute of Physics. [doi:10.1063/1.3630000]

The  $\text{In}_x\text{Ga}_{1-x}\text{N}$  (IGN) system is a suitable candidate for the development of blue and green light emitting diodes as well as laser diodes. The band gap of IGN alloy system can be tuned from infrared (0.7 eV for InN) to ultraviolet (3.4 eV for GaN) by changing the indium composition. It has been well reported that as grown InN always exhibits  $n$ -type conductivity with unintentional free electrons with concentrations as high as  $10^{21} \text{ cm}^{-3}$ .<sup>1,2</sup> The  $n$ -type conductivity in InN is mainly attributed to the donor levels created by impurities such as hydrogen and oxygen and the presence of native defects like nitrogen vacancies.<sup>3</sup> Recently, Biju *et al.*<sup>4,5</sup> have proposed a room temperature growth technique known as modified activated reactive evaporation (MARE) for the growth of group-III nitrides. Since MARE is a room temperature growth technique, the undoped IGN films prepared by this are expected to have large number of nitrogen vacancies which may result in high background carrier concentration. Lin *et al.*<sup>6</sup> have studied the electron transport in indium rich IGN films and have found them to be degenerate semiconductor systems with a metal like electron transport behavior. Yildiz *et al.*<sup>7</sup> have observed a metal-semiconductor transition at  $\sim 180$  K for IGN films with  $x=0.17$ . There is a definite need to study the metal to semiconductor transition and other transport properties in the entire composition range for IGN alloy films.

In the present study, low temperature ( $10 \text{ K} \leq T \leq 300 \text{ K}$ ) carrier transport studies has been carried out on  $\text{In}_x\text{Ga}_{1-x}\text{N}$  thin films ( $0.12 < x < 0.93$ ) grown by MARE technique. The temperature dependent resistivity has been explained using the metallic conduction model. The semiconducting behavior has been analyzed by taking into account consideration the electron-electron interaction (EEI) and weak localization (WL).

IGN films were prepared on borosilicate glass substrates by MARE technique. The details of the MARE technique are discussed in our earlier works.<sup>8,9</sup> The thickness of all the IGN

films was found to be varying from 600 to 800 nm as determined from reflectance spectra using Filmetrics F20 spectrophotometer. The scanning electron micrographs were recorded using a field emission scanning electron microscope (FESEM) FEI Quanta 200 with an energy dispersive X-ray (EDX) detector attached to it. Further information regarding the surface morphology was studied using Digital Instruments Nanoscope IV atomic force microscope (AFM) in contact mode.

The low temperature resistivity and Hall measurement studies were carried out in van der Pauw geometry for all the IGN films. Ohmic contacts were given to  $5 \times 5 \text{ mm}^2$  square samples at the four corners using annealed indium dots. Measurements were made over the temperature range of 10–300 K with steps of 10 K using a Lake Shore (7600 series) Hall effect measurement system. At each temperature step, the Hall coefficient (with maximum 5% error) and resistivity (with maximum 0.2% error) were measured for both the current directions at an average magnetic field of 4.5 kG.

From the X-ray diffraction (XRD) pattern (Fig. 1(a)), it was observed that all the films are polycrystalline in nature with preferential growth along the  $c$ -axis without any traces of metallic indium or gallium. For some of the gallium rich

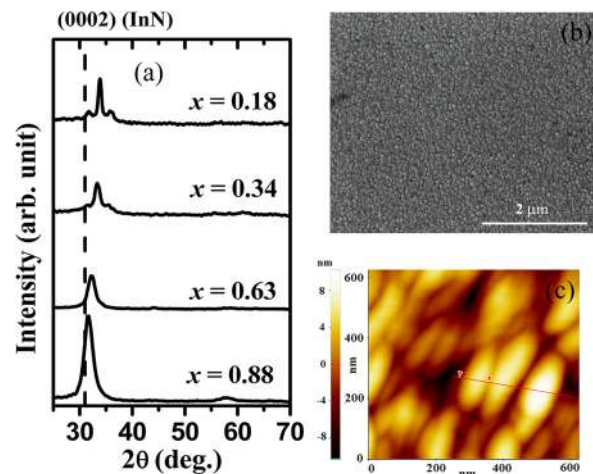


FIG. 1. (Color online) (a) XRD pattern of IGN films, (b) FESEM image for  $x=0.63$  film, and (c) AFM image for  $x=0.75$  film.

<sup>a)</sup>Present address: Department of Physics, Government College Kodenchery, Calicut-673580, India.

<sup>b)</sup>Electronic mail: mkj@physics.iit.ac.in.

films weak shoulder peaks corresponding to (10 $\bar{1}$ 0) and (10 $\bar{1}$ 1) orientations were observed. The indium composition determined from (0002) XRD peak shift using Vegard's law was found to vary from 12 to 93% for different IGN films. This was in good agreement with the compositions obtained from EDX analysis. The phase segregation<sup>9</sup> was observed in the composition range  $0.44 < x < 0.60$ . The FESEM image for  $x=0.63$  IGN film shows polycrystalline nature of the films with an average grain size of 54 nm (Fig. 1(b)). The AFM micrograph of  $x=0.75$  IGN film (Fig. 1(c)) shows the tilted grains, which is mainly due to the glancing angle deposition involved during the evaporation process. From the SEM as well as AFM images it was further verified that there are no indium or gallium metallic cluster formation at the growth front. The optical band gap values obtained from transmittance spectra were found to vary from 1.9 to 3.0 eV.

Fig. 2(a) shows the temperature dependent carrier concentrations for the IGN films. Due to instrumental limitation, reliable Hall effect measurements to determine the carrier concentration of the highly resistive  $x=0.12$  film was not possible especially at lower temperatures where the resistivity increases sharply. All the studied films were found to exhibit  $n$ -type conductivity. The carrier concentration was found to be increasing with increase in indium concentration in the films. For all the studied compositions ( $x > 0.12$ ), the carrier concentration was independent of temperature within the experimental error. This implies that the Fermi level for IGN samples in the present investigation lies above the

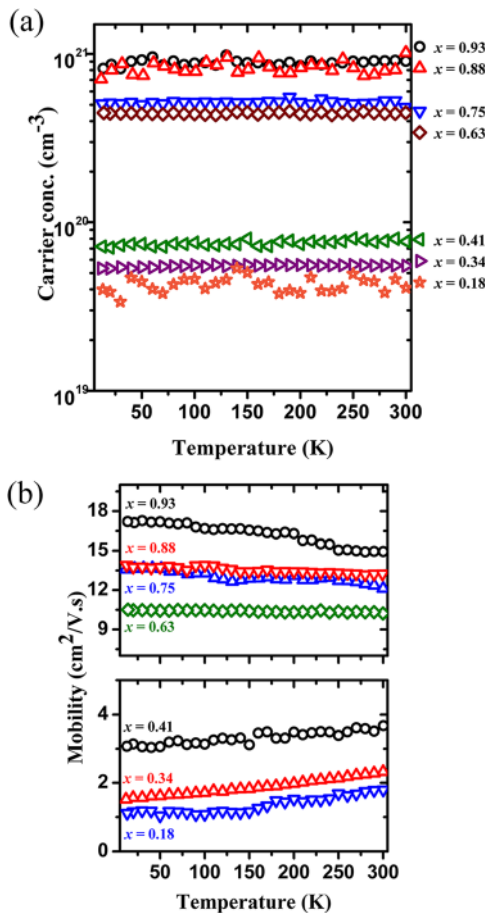


FIG. 2. (Color online) Temperature dependent (a) carrier concentration and (b) mobility values of IGN films with different indium concentrations.

conduction band bottom.<sup>10</sup> Hence, the IGN films can be considered as degenerate electron systems in the measured temperature range. For the degenerate semiconductors, the Coulombic interaction between the electrons is very high which leads to a reduction in the electron mobility values (Fig. 2(b)). Again, grain boundary scattering also contributes to the reduction in the mobility values due to the polycrystalline nature of the films. The temperature dependent scattering mechanism in IGN thin films is the combined result of electron-electron scattering, ionized impurity scattering ( $\mu \propto T^{3/2}$ ), alloying effect ( $\mu \propto T^{-1/2}$ ),<sup>11</sup> scattering by acoustic phonons ( $\mu \propto T^{-3/2}$ ), and scattering by optical phonons ( $\mu \propto T^{-1/2}$ ). The mobility values for all the films were found to be nearly temperature independent within the experimental error which is the characteristic of a weakly disordered system.

Fig. 3 shows the temperature dependent resistivity of IGN films for all the compositions. Metallic behavior was found to be prominent for indium rich films. With gallium incorporation, the carrier concentration decreases resulting in a metal to semiconductor electronic phase transition (MST) at lower temperatures ( $\sim 150$  K) for the films with  $x=0.88$  and  $0.75$ . With further increase in gallium concentration, semiconducting behavior was observed in the whole temperature range.

From the temperature dependent carrier concentration, mobility, and resistivity plots, it is clear that the electron transport in these degenerate semiconductors is mainly controlled by the impurity band conduction. Therefore, we cannot use the classical Arrhenius equation ( $\rho(T) = \rho_0 \exp(E_a/k_B T)$  where  $E_a$  is the corresponding activation energy) to explain the transport phenomena. Thus, we need to implement quantum corrections to conductivity for the correct interpretation of the resistivity plots. The quantum corrections include the WL effect and EEs.<sup>12–14</sup> In order to understand the transport properties, the resistivity curves were fitted to the following expression<sup>15,16</sup>:

$$\rho(T) = \frac{1}{\sigma_0 + mT^{1/2} + BT^{p/2}} + kT^2. \quad (1)$$

Here,  $\sigma_0$  is the residual conductivity (Boltzmann conductivity) and  $mT^{1/2}$  corresponds to the Coulombic electron interactions renormalized by self-interference effects (Altshuler-Aronov correction). The term  $BT^{p/2}$  describes the weak localization due to the self-interference of quantum wavefunctions backscattered on impurities, in which  $p$  depends on the nature of interaction ( $=2$  or  $3$  for electron-electron or electron-phonon interactions, respectively). In addition to the quantum corrected resistivity, a term  $T^2$  is included to account for higher temperature scattering contributions. The fitted curves are shown as solid lines in Fig. 3. For  $x=0.63$ ,  $0.41$ ,  $0.34$ , and  $0.18$  IGN films, the resistivity curves were fitted in two different temperatures regimes i.e., (10–150 K) and (150–300 K). In general, the quantum corrections are incorporated at very low temperatures ( $< 10$  K). But for wide band gap degenerate semiconductors like IGN and ZnO, quantum corrections to resistivity at temperatures as high as 300 K have been reported.<sup>7,16</sup> The best fit for all the samples were obtained when the parameter  $p$  was fixed at 2. This

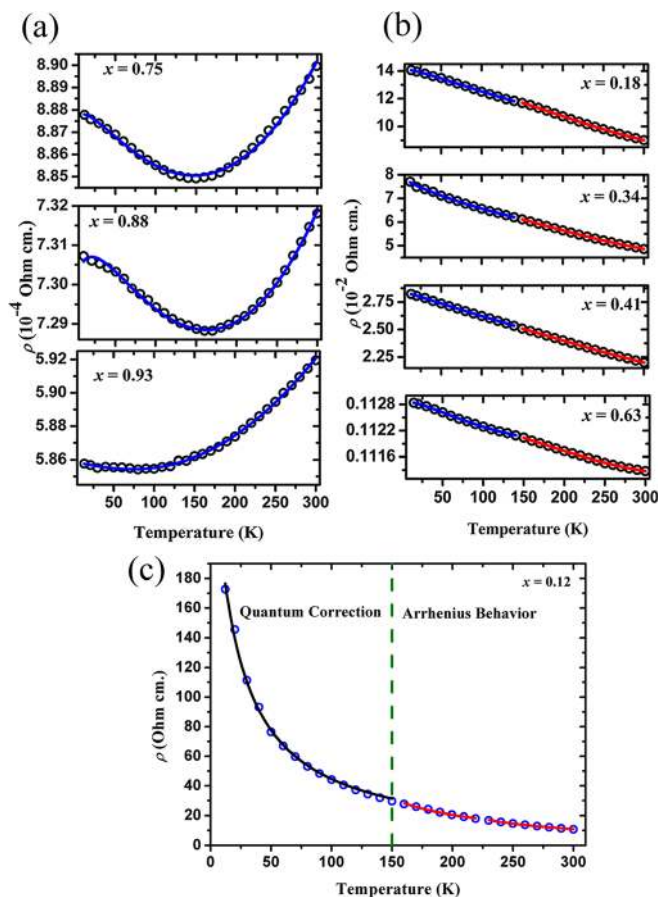


FIG. 3. (Color online) Temperature dependent resistivity of IGN films (Solid lines show the theoretically fitted curves).

means that electron-electron interaction plays the dominating role in the transport mechanism. The negative  $m$  values<sup>17,18</sup> obtained from fitting show the existence of dominant metallic behavior in IGN samples. The quantum corrections given by WL and EEI decreases with increase in temperature, leading to a decrease in resistivity which accounts for the semiconducting behavior observed in all the films. However, for IGN films with  $x \geq 0.75$  (Fig. 3(a)), the electron-phonon scattering dominates at higher temperatures resulting in an increase in resistivity with increase in temperature. This accounts for the metallic type behavior exhibited by these indium rich films at higher temperatures.

The temperature dependent resistivity plot for  $x = 0.12$  film is shown in Fig. 3(c). Here, we can observe a transition from the quantum corrected resistivity behavior to the classical

Arrhenius behavior above 150 K. The corresponding activation energies in the temperature range (160–220 K) and (220–300 K) were found to be 22.06 and 37.9 meV, respectively. Below 150 K, small quantum effects are observed with the WL term  $B \sim 10^{-4} (\Omega \text{ cm K})^{-1}$ .

Below room temperature (10–300 K) carrier transport studies for IGN films in the entire composition range were carried out. Temperature independent carrier concentration and low mobility values in these films clearly indicate the existence of a metallic impurity band. An MST at  $\sim 150$  K for  $x = 0.88$  and 0.75 IGN films was observed. The gallium rich films show semiconducting behavior in the entire temperature range. The semiconducting behavior is explained by employing quantum corrections to conductivity involving WL and EEI effects. For  $x = 0.12$  films a transition from quantum corrections to classical Arrhenius behavior was observed at 150 K.

<sup>1</sup>L. F. J. Piper, T. D. Veal, C. F. McConville, H. Lu, and W. J. Schaff, *Appl. Phys. Lett.* **88**, 252109 (2006).

<sup>2</sup>A. G. Bhuiyan, A. Hashimoto, and A. Yamamoto, *J. Appl. Phys.* **94**, 2779 (2003).

<sup>3</sup>C. G. Van de Walle, J. L. Lyons, and A. Janotti, *Phys. Status Solidi A* **207**, 1024 (2010).

<sup>4</sup>K. P. Biju, A. Subrahmanyam, and M. K. Jain, *J. Phys. D: Appl. Phys.* **41**, 155409 (2008).

<sup>5</sup>K. P. Biju, A. Subrahmanyam, and M. K. Jain, *J. Cryst. Growth* **311**, 2275 (2009).

<sup>6</sup>S. K. Lin, K. T. Wu, C. P. Huang, C. T. Liang, Y. H. Chang, Y. F. Chen, P. H. Chang, N. C. Chen, C. A. Chang, H. C. Peng, C. F. Shih, K. S. Liu, and T. Y. Lin, *J. Appl. Phys.* **97**, 046101 (2005).

<sup>7</sup>A. Yildiz, S. B. Lisesivdin, M. Kasap, and M. Bosi, *Solid State Commun.* **149**, 337 (2009).

<sup>8</sup>K. P. Biju and M. K. Jain, *Appl. Surf. Sci.* **254**, 7259 (2008).

<sup>9</sup>S. R. Meher, K. P. Biju, and M. K. Jain, "Raman spectroscopic investigation of phase separation and compositional fluctuations in nanocrystalline  $\text{In}_x\text{Ga}_{1-x}\text{N}$  thin films prepared by modified activated reactive evaporation", *Phys. Status Solidi A* (to be published).

<sup>10</sup>I. Mahboob, T. D. Veal, C. F. McConville, H. Lu, and W. J. Schaff, *Phys. Rev. Lett.* **92**, 036804 (2004).

<sup>11</sup>C. Wang, N. Maeda, K. Tsubaki, N. Kobayashi, and T. Makimoto, *Jpn. J. Appl. Phys.* **43**, 3356 (2004).

<sup>12</sup>P. A. Lee and T. V. Ramakrishnan, *Rev. Mod. Phys.* **57**, 287 (1985).

<sup>13</sup>C.-T. Liang, C. G. Smith, J. T. Nicholls, R. J. F. Hughes, M. Pepper, J. E. F. Frost, D. A. Ritchie, M. P. Grimshaw, and G. A. C. Jones, *Phys. Rev. B* **49**, 8518 (1994).

<sup>14</sup>P. P. Edwards, R. L. Johnston, C. N. R. Rao, D. P. Tunstall, and F. Hensel, *Philos. Trans. R. Soc. London, Ser. A* **356**, 5 (1998).

<sup>15</sup>G. A. Thomas and A. Kawabata, *Phys. Rev. B* **26**, 2113 (1982).

<sup>16</sup>M. Nistor, F. Gherendi, N. B. Mandache, C. Hebert, J. Perriere, and W. Seiler, *J. Appl. Phys.* **106**, 103710 (2009).

<sup>17</sup>C. Leighton, I. Terry, and P. Becla, *Phys. Rev. B* **58**, 9773 (1998).

<sup>18</sup>A. Yildiz, S. B. Lisesivdin, P. Tasli, E. Ozbay, and M. Kasap, *Curr. Appl. Phys.* **10**, 838 (2010).